

Aggregation dynamics of active cells on non-adhesive substrate

Debangana Mukhopadhyay¹, Rumi De^{1*},

Department of Physical Sciences, Indian Institute of Science Education and Research
Kolkata, Mohanpur 741246, India.

E-mail: rumi.de@iiserkol.ac.in

December 2018

Abstract. Cellular self-assembly and organization are fundamental steps for the development of biological tissues. In this paper, within the framework of a cellular automata model, we address how an ordered tissue pattern spontaneously emerges from a randomly migrating single cell population without the influence of any external cues. This model is based on the active motility of cells and their ability to reorganize due to cell-cell cohesivity as observed in experiments. Our model successfully emulates the formation of nascent clusters and also predicts the temporal evolution of aggregates that leads to the compact tissue structures. Moreover, the simulations also capture several dynamical properties of growing aggregates, such as, the rate of cell aggregation and non-monotonic growth of the aggregate area which show a good agreement with the existing experimental observations. We further investigate the time evolution of the cohesive strength, and the compactness of aggregates, and also study the ruggedness of the growing structures by evaluating the fractal dimension to get insights into the complexity of tumorous tissue growth which were hitherto unexplored.

1. Introduction

Formation and development of tissues through self-assembly and organization of living cells are intriguing and complex phenomena [1, 2]. It is still not well understood how ordered tissue structures spontaneously develop from orchestrated response of interacting multi-cellular components. Understanding the process of tissue organization, thus, would immensely benefit diverse areas of developmental biology, wound healing, cancer therapy, tissue engineering and even organ printing to name a few [1–9].

In nature, numerous examples of self-assembled aggregation processes can be found both in living as well as non-living systems [10], such as, formation of snowflakes [11], cloud formation [12], coagulation of colloids [13], aggregation of proteins [14], swarming of bacteria [15–17], flocking of birds [18] etc. Several experimental, theoretical, and computer simulation studies have been carried out which reveal a great deal about the structural and dynamical aspects of self-assembly and aggregation processes in passive systems [19, 20]. For an example, studies on diffusion-limited aggregations

provide a deep understanding into the process of snowflakes like branched dendritic patterns formation [21–25]. Moreover, it has been found that variety of inter-particle interactions, reaction mechanisms, coalescence rates, and other factors play a crucial role in determining the dynamics of aggregates [19, 20].

There have also been many efforts to understand the assembly and organization processes of living tissues, such as, how tissues spread [26–28], how sorting takes place in a multicellular system [29–32], or how tumors develop and grow [4, 33]. An insight into the complex tissue organizations could be obtained based on differential adhesion hypothesis (DAH) proposed by Steinberg *et. al.* [34–36]. According to DAH, motile and cohesive cells spontaneously tend to reorganize to maximize cell-cell cohesive binding strength and to minimize the interfacial energy of aggregates. DAH, thus, provides an important route to the formation of ordered tissue patterns from collective interactions of multi-cellular components. There are also quite a few theoretical and computational studies to understand the complex behaviours of tissues, for examples, Graner and Glazier have developed theoretical model to investigate the phenomenon of cell sorting [31]; Sun and Wang’s group have simulated fusion of multicellular aggregates [37]; Flenner *et. al* have modelled temporal shape evolution of multicellular systems [30]. Moreover, reaction-diffusion mechanisms have also been shown to influence the formation of many tissue patterns, such as rapidly growing embryo or stem cell aggregate [1], aggregation of amoebae motion [38].

Interestingly, in recent experiments, performed by Douezan and Brochard-Wyart, it has been observed that randomly migrating cells deposited on non-adhesive surface spontaneously form closely packed compact aggregates [7]. There are other experiments which also exhibit the tendency of cellular aggregates to spontaneously form compact tissue structures acquiring minimum area [28, 39–42]. Examples include, rounding up of Hydra aggregates into circular shapes in 2D [43] or chick embryonic cellular aggregates evolving into spherical shapes in 3D [44]; in all these cases, cell-cell adhesion bonds have been found to play a significant role in shaping up the structure. A key step to get insights into these processes is to understand what drives cell-cell attraction to form compact multi-cellular aggregates. Several hypotheses have been proposed, in particular, whether cell-cell attraction is based on chemical signalling [45] or whether cellular communications are mediated by extracellular matrix - where deformations created in the substrate by one cell can be detected by an adjacent cell [46], or the attraction is mediated due to haptotaxis, i.e., directional cell motility up a gradient in the substrate [47]. Motivated by the experimental findings, in this paper, we address how an ordered tissue pattern spontaneously emerges from a seemingly disordered single cell population without the influence of any external physical or chemical forces. We show that a suitably constructed cellular automata model based on the active motility and local reorganization of cells can successfully capture the formation of nascent clusters and predict the temporal evolution of aggregates that leads to the compact tissue structures as observed in experiments. The crux of our model is that the sole consideration of the cellular tendency of forming bonds with neighbouring cells to maximize cohesive

strength, is sufficient for the emergence of compact tissue pattern. Our study thus shows that the presence of an external cue or a mediator or a gradient is not critical to these types of aggregations which was hitherto unexplored. Our theory also reveals the existence of two distinct time scales in such cellular aggregation processes - one is fast time scale associated with the diffusion of cells and another much slower time scale associated with the tissue compaction process that involves breaking of cell-cell cohesive bonds and making of new bonds. Interestingly, we find that the difference in the tendency of cell types to self-organize to increase the binding strength plays a crucial role in determining the time scale and the structure of the tissue pattern.

Apart from emulating the structural evolution, our model also captures several dynamical properties of cellular aggregates [4, 7, 28], such as, the rate of aggregation, *i.e.*, how the number of cell clusters evolve with time as the aggregation takes place. Moreover, as observed in experiments, our model also predicts the non-monotonic growth of the surface area of the growing aggregates on non-adhesive substrates. We further investigate, how the cellular cohesive binding strength and the overall compactness of the growing aggregate evolve as time progresses which remains so far unexplored. Besides, we also study how the ruggedness of the growing aggregate structure changes towards a smooth compact structure by evaluating the fractal dimension of the aggregate which can be useful in comparing normal versus decreased tissue growth as revealed by the recent experiments [48, 49].

2. Cellular automata modelling

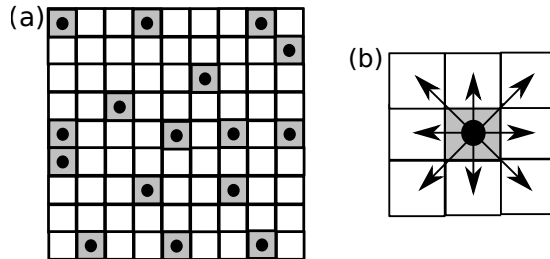


Figure 1. (a) Illustration of randomly deposited cells on a lattice surface. Shaded areas represent lattice sites occupied by cells and each dot represents the center of mass of the cell. (b) Schematic of eight neighbouring sites of a cell.

In this section, we now discuss the formulation of our cellular automata model in details. First, we start with N_0 cells randomly deposited on a $(L \times L)$ square lattice as illustrated in Fig. 1(a). Each lattice site is, thus, either occupied by a cell or remains empty. Each cell is considered to have eight nearest neighbouring sites as depicted in Fig. 1(b) to form a close packed structure in a square lattice. In our model, cells can diffuse to any of its empty neighbouring sites. On the way, if it finds another immediate neighbouring cell then sticks to it due to cell-cell binding affinity and starts moving

together as a whole cluster. Here, the sticking probability is considered to be 1. Thus, at any instant, there are $N(t)$ number of cell clusters. It is to be noted that, in our simulation, we refer a single cell also as a cluster. Thus, a cluster can consist of a single cell or multiple cells. In our model, at each simulation step, $N(t)$ clusters are picked up at random one by one and then the cluster is given the opportunity to (i) either diffuse with a motility probability, $P_m(n)$, (ii) or locally reorganize with a rolling probability, $P_r(n)$, within its own cluster so that cell-cell cohesive binding strength increases, (iii) otherwise, just stay put.

Motility criteria: The motility probability of a cluster is considered to be dependent on its size as $P_m(n) = \frac{\mu}{n}$; where n is the number of cells in the cluster and μ is the proportionality constant. In our simulations, μ is taken as 1. As time progresses, diffusing clusters collide and merge to form a bigger cluster. Thus, the motility of the cluster decreases with accumulation of more number of cells. The dependence of the probability, $P_m(n)$ on $1/n$ could simply be attributed to the decreasing tendency of diffusion of the cluster as it gathers more mass, since the diffusion coefficient, $D \propto \frac{1}{m}$; where m is the mass to the cluster and hence, proportional to the number of cells, n , of the cluster [50]. Moreover, as found in experiments, the cluster motility gradually slows down with increase in size and eventually stops moving after it reaches a critical size (say, n_c number of cells).

Local reorganization: Now, we discuss in detail the local reorganization of cells within its own cluster via rolling process. As cells in a cluster are bound together by strong cell-cell adhesion, local reorganization process requires breaking of existing cell-cell cohesive bonds and again making of new bonds. Thus, this process is observed to be much slower process compared to diffusion. Therefore, in our model, we consider an additional probability factor, $P_r(n) = \beta n$ to incorporate the slower compactification process, where the rolling parameter β denotes the tendency of the cell type to locally reorganize due to the binding affinity. The cell rearranges its position relative to the neighbouring cells so that it is surrounded by the maximal possible neighbours and hence, increases the cell-cell binding strength. As the cluster size gets bigger, probability of rolling increases with increase in number of cells, n , in the cluster.

In our model, the cell-cell binding interaction energy is described as,

$$E = -\epsilon_1 n_1 - \epsilon_2 n_2 - \epsilon_3 n_3; \quad (1)$$

where n_1, n_2 , and n_3 are the number of first, second and third nearest neighbouring cells and ϵ_1, ϵ_2 , and ϵ_3 are the weight factors given to its neighbouring binding sites respectively. Here, we assume that the interaction strength between a cell and its first nearest neighbours is maximum as they are adjacent to each other and the interaction strength gradually decreases from second to third neighbours. It is also observed in experiments that cell-cell interaction can extend beyond first nearest neighbours, since apart from the physical contact, cell-cell attraction could be driven by chemical signalling i.e. cells secrete chemoattractants into the medium.

Now, at each simulation step, for a randomly chosen cluster, if the motility criteria,

$P_m(n)$, are not satisfied, then we check for the rolling probability criterion, $P_r(n)$. Once it is satisfied then we check whether the local reorganization can take place. We, first, calculate the binding interaction energy, E_0 , of the cell in its current location following Eq. (1). Next, we choose randomly an empty 1st nearest neighbouring site for its possible relocation and calculate its binding energy, E_n , at the new position. If the corresponding binding energy, E_n , associated with the new location is lowered compare to its current configuration, E_0 , so that it leads to an over all increase of cellular binding strength due to more cell-cell interactions, then the move is readily accepted. However, if the energy, E_n , becomes higher, then a random number, r , is generated from the uniform distribution over the interval $[0, 1]$, and the new configuration is accepted with a probability such that $r < \exp(-\Delta E)$, where $\Delta E = E_n - E_0$, is the corresponding change in cellular interaction energy. In simulations, we have considered, $\epsilon_1 = 3$, $\epsilon_2 = 2$, and $\epsilon_3 = 1$.

2.1. Numerical algorithm

Details of numerical steps of our cellular automata model are summarized as follows:

- (i) N_0 cells are, initially, deposited at random on a $L \times L$ two dimensional square lattice as shown in Fig. 1(a). (As single cell is also referred as a single cell cluster; thus, initially, the number of clusters, $N(t) = N_0$.)
- (ii) At each simulation step, $N(t)$ clusters are randomly picked up one by one (once a cell of a cluster is randomly chosen, no other cells of that particular cluster will be chosen at that step). Then, we record the number of cells, n , of the chosen cluster. Next, we check whether the motility or the local reorganization or the stay put criterion of the cluster is satisfied.
- (iii) Motility criteria: a random number R_1 is generated from the uniform distribution over the interval $[0, 1]$. If $R_1 \leq P_m(n) = \frac{1}{n}$ and the size of the cluster is less than a critical number n_c , then the whole cluster moves in any of the empty first nearest neighbouring sites.
- (iv) Criteria of local rearrangement : if the motility criteria are not satisfied then we check for the rolling criteria. We call another random number R_2 and if $R_2 \leq P_r(n) = \beta n$, then the chosen cell of that cluster given an opportunity to locally rearrange within its own cluster to be surrounded by more number of neighbours.
- (v) Now, for reorganisation process to occur, an empty site in its first nearest neighbouring region is randomly chosen. Then, we calculate the binding energy, E_n , in its possible new location and the energy, E_0 , in its current location. If $E_n \leq E_0$, the new location is readily accepted. Otherwise, if $E_n > E_0$, then we call a random number (r) from a uniform distribution $[0, 1]$, if $r < \exp(-\Delta E)$ where $\Delta E = E_n - E_0$, then the move is accepted except if the move disintegrates the cluster then that move is not allowed (as illustrated in Figure ??(a) & (b) in supplementary information).

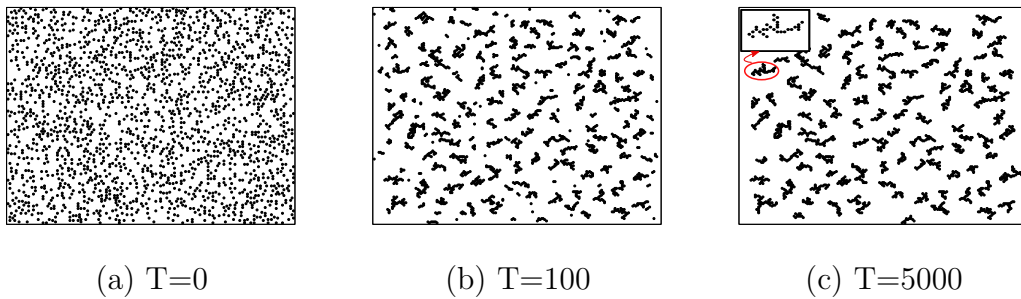


Figure 2. Time evolution of diffusion limited aggregation of cells. (a) Presents a snapshot at simulation time $T = 0$, here 2000 cells are deposited randomly on (200×200) lattice surface. (b) While diffusing, cells collide and stick to each other to form aggregates, one such snapshot at $T = 100$. (c) Shows irregular branched cellular aggregates at $T = 5000$. The inset focuses one such irregular shaped cell aggregate.

- (vi) If both the motility and the rolling criteria are not satisfied, then the cluster just stays put.

3. Results and discussions

We now investigate the dynamics of initiation, growth, and evolution of cellular aggregates on non interacting surface following the cellular automata model described in the previous section. In our simulations, we start from a population of randomly distributed single cells spread over a 2D surface. While diffusing on the surface, cells collide, stick to each other, and thus form small nascent clusters of two or three cells clusters. These clusters then grow with accumulation of more colliding cells or clusters and give rise to large aggregates. Our simulations capture many dynamical properties of growing aggregates, those we discuss in detail in the following subsections. We have performed simulations for a wide range of parameter values and results presented here after averaging over many such simulations.

3.1. Aggregation of cells due to diffusion

We, first, study the effect of simply diffusion into the aggregation of cells. The time evolution of cell aggregation due to diffusion is shown in Figs. 2(a)-(c). Figure 2(a) shows the initial deposition of 2000 cells on a 200×200 lattice. These cells diffuse to any of its empty first nearest neighbouring sites with a probability $P_m(n) = \mu/n$. On the way, when they come across with other cells or clusters, they stick irreversibly and form bigger clusters. Figure 2(b) shows such an intermediate time step of clustering of cells. As time progresses, these clusters grow with gathering of more diffusing clusters. However, the cluster motility gradually slow down with increase in cluster size and eventually stop moving after reaching a critical size, n_c , as observed in experiment [7]. Figure 2(c) presents a snapshot of cellular aggregates acquiring irregular branched structures as predicted by diffusion limited aggregation studies [21–23]. The irregular shapes arise,

since the diffusing cells/clusters only access the protruding exterior regions as they irreversibly stick to the immediate neighbours, thus, do not roll down to the interior of the cluster. Simulation results are presented here for $n_c = 10$ as the critical size of the cluster is found of the order of ten in experiment [4, 7]. We have also carried out simulations with $n_c = 20$ and 30; the size of aggregates becomes bigger and develops more branched structure; however, the qualitative nature of aggregates remains the same.

3.2. Aggregation: effect of local reorganisation of cells

Next we investigate, in addition with diffusion, the influence of local reorganization of cells due to strong cell-cell binding affinity on the dynamics of aggregate formation. As observed in experiments, aggregates are grown generally compact in nature, where, cell-cell interaction to increase the cohesive binding strength plays a crucial role in smoothening out the irregular structures. We start with $N_0 = 2000$ cells placed randomly on 2D square lattice of size $L = 200$. In this case, cells or clusters may diffuse with a probability, $P_m(n) = \mu/n$, otherwise may opt to locally reorganize with a rolling probability, $P_r(n) = \beta n$ or just stay put as described in the previous section. Figures 3(a)-(c) present one such simulation results of temporal evolution of aggregates formation (keeping $\mu = 1$ and $\beta = 0.05$). From these figures, it is clearly seen that as time progresses, aggregates grow in size and also gradually become compact due to local rearrangements of clustering cells. After a sufficiently long time, aggregates become fully compact and one such compact structure is shown in the inset of Fig. 3(c).

Moreover, we have carried out simulations for different cell density, $\rho = N_0/(L \times L)$, (keeping $N_0 = 500, 1000, 2000, 10000$, and $L = 200$) and studied the effect of varying density in the formation of cellular aggregates. Under low densities, cells/clusters diffuse for longer time to find another cell or cluster to bind together and hence, the clustering

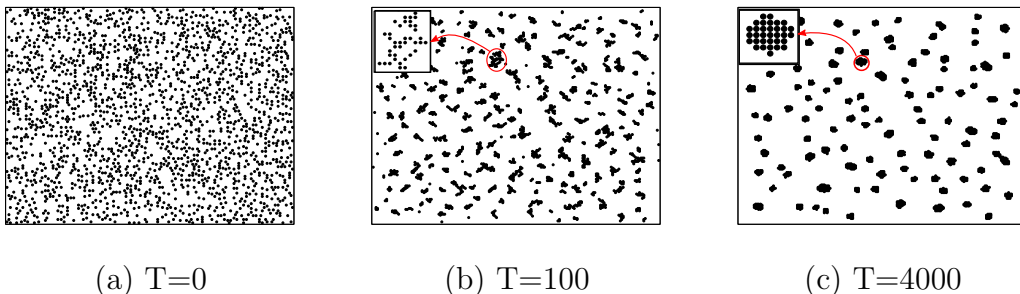


Figure 3. Time evolution of aggregates formation due to diffusion and local reorganizations of cells. (a) Presents a snapshot of random deposition of 2000 cells on a (200×200) lattice at simulation time $T = 0$. (b) A snapshot of growing aggregates at $T = 100$. Clusters initially grow as irregular shaped structure as shown in the inset. (c) Shows compact cellular aggregates after a sufficiently long time at $T = 4000$. The compact shape develops due to rearrangement of clustering cells to maximize the binding strength. The inset shows such a compact cell aggregate. (Results presented here for $n_c = 10$ and $\beta = 0.05$.)

process also takes longer time. However, for higher densities, diffusing cells find other cells in its immediate vicinity. So, the growth process becomes faster and the cluster size also gets bigger due to availability of more number of cells. On the other hand, having a large cluster size, local cell-cell rearrangements take longer time and thus, the overall compactification process becomes slower. Moreover, the compactification time strongly depends on the nature of cell types, cellular tendency of making and breaking adhesion bonds etc., in our simulations, which is represented by the variation in rolling coefficient, β . We discuss these properties of the cellular aggregation in more details in the following subsections.

3.3. Rate of cell aggregation

In this section, we investigate the rate of aggregation, *i.e.*, number of clusters formation as a function of time. Clusters mainly form due to the random collisions of diffusing clusters. Thus, at any instant, if there are $N(t)$ number of clusters of single cell or multiple cells, then the occurrence of number of collisions for one cluster is $(N - 1)$ as there are other $(N - 1)$ surrounding clusters. Thus, at any time instant t , since all clusters randomly move and collide with other; so the total number of collisions considering all clusters movement is proportional to $N(N - 1)$. Thus, the time evolution of the number of clusters can be described by the equation,

$$\frac{dN(t)}{dt} = -KN(t)(N(t) - 1) \approx -KN(t)^2, \quad (2)$$

where K is the rate constant which depends on the size and motility of the cell type. [7]

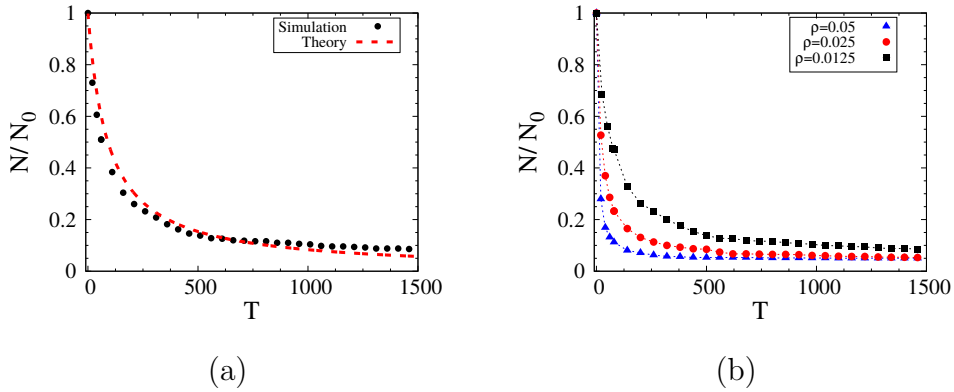


Figure 4. Time evolution of number of clusters.(a) Comparison of simulation result of rate of aggregation (\bullet), keeping $\rho = 0.0125, \beta = 0.05$) with theoretical model prediction, solution of Eq. 2, shown by the dashed curve. (b) Formation of number of aggregates as a function of time for different initial cluster density, $\rho = 0.0125$ (\blacksquare), 0.025 (\bullet), and 0.05 (\blacktriangle).

From our simulation, we evaluate the rate of cell aggregation, *i.e.*, the rate of change of number of clusters during the aggregation process. We find as the clusters while diffusing collide with each other and merge to form bigger aggregates and hence, the

number of clusters decreases with time. Besides, since the aggregate stops moving after reaching a critical size (as its mass gets heavier), number of clusters eventually reaches to a steady value. Figure 4(a) shows our simulation results of time evolution of number of clusters which is in good agreement with recent experimental observations [7] (as it is also seen from Figure ?? provided in the supporting information). We also compare our simulation results with the theoretical prediction of Eq. (2). As seen from Fig. 4(a), the theoretical prediction agrees quite well with our simulations as well as with the experimental observations by tuning only one fitting parameter, the rate constant K .

Moreover, we also study the effect of cell density variation on the rate of cell aggregation. Figure 4(b) shows the simulation results for three different densities $\rho = 0.0125, 0.025, \text{ and } 0.05$ (with initial cell number, $N_0 = 500, 1000, 2000$ and $L = 200$). As shown in Fig. 4(b), for higher density, the decrease in the number of clusters is faster; since chances of finding neighbouring cells/clusters are higher, the rate of merging of clusters is also high. In other words, the growth of aggregates happens faster for higher cell density.

3.4. Evolution of surface area of an aggregate

Recent experimental studies show that the surface area of the growing aggregates on non-adhesive substrate exhibits a non-monotonic evolution unlike the monotonic increase in the area as observed in case of spreading of cell aggregates [27]. In order to get an insight into the dynamics, we also investigate the area evolution of the aggregates. In our simulations, we consider two methods to estimate the surface area of an aggregate. In one method, we calculate the perimeter of the cluster, which in turn provides an estimation of the projected area and in another, we calculate the radius of gyration of the cluster to evaluate the surface area (details have been given as supporting materials).

We have studied the time evolution of the surface area averaged over many aggregates for different cell density, $\rho = 0.0125, 0.025, 0.05$ and rolling tendency of varied cell type given by $\beta = 0.0005, 0.005, 0.05$ as shown in Figure 5 (a) and 5(b) respectively. We find, as observed in experiment, [7] at the early stages of the growth process, the surface area of the cluster increases rapidly due to collisions and merging of clusters. However, once the aggregate reaches a critical size, it stops moving and other than occasional joining of randomly wandering of small clusters, the cells reorganize among themselves to be surrounded by the maximum possible neighbours, and hence, the surface area start decreasing due to the compactification process and finally reaches to a steady state value giving rise to the most compact structure. Insets of Fig. 5 (a) show an irregular shaped structure that arises due to joining of diffusing cells at early times and a compact structure due to self-organization of the clustering cells at a longer period of time. Importantly, our model could capture the non-linear nature of the cluster area evolution as found in experiments which could also be seen from Figure ?? in the supplementary information.

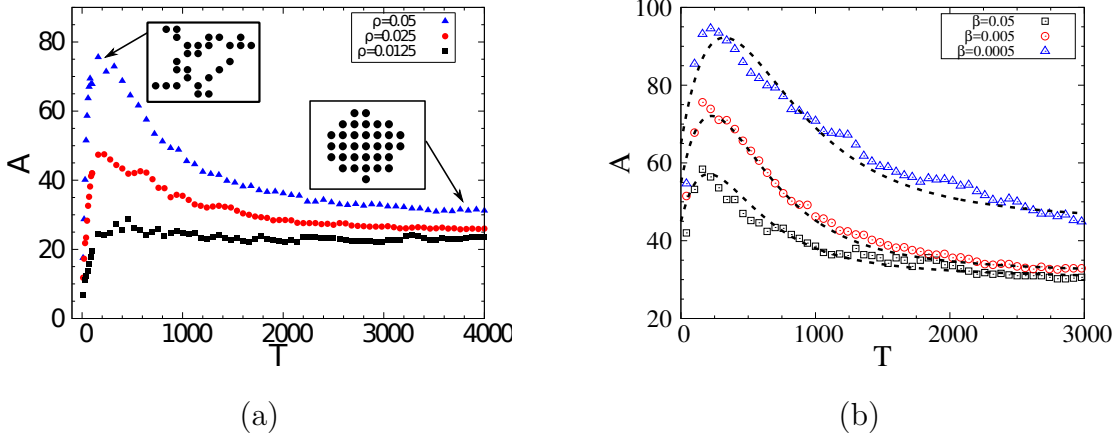


Figure 5. Time evolution of the surface area of cellular aggregate (a) Simulation results for different initial cluster density, $\rho = 0.0125$ (■), 0.025 (●), 0.05 (▲). Left panel inset shows the development of irregular shaped structure at some initial time and right panel inset shows the compactified structure at a longer period of time. (b) Shows the effect of rolling coefficient on the surface area evolution for $\beta = 0.0005$ (▲), 0.005 (○), and 0.05 (□). Theoretical prediction, solution of Eq. (3), is shown by the dashed curve (τ_c has been varied for different β values and while keeping K constant).

The time evolution of the cluster area, $A(t)$, during the aggregation process can also be theoretically modeled following earlier studies [39, 40] as,

$$\frac{dA(t)}{dt} = KN(t)A(t) - \frac{1}{\tau_c}[A(t) - A_{final}]; \quad (3)$$

where $N(t)$ is the number of clusters at any instant t . Here, the first term represents the area increase due to diffusive collision and merging of clusters and the second term represents the decrease in area with a characteristic relaxation time, τ_c , which is related to the tendency of reorganization of cells to reach to the most compact structure of an area A_{final} .

We now compare simulation results of our cellular automata model with the theoretical prediction. We numerically solve Eq. (3) substituting $N(t)$ from Eq. (2) keeping K constant and varying values of τ_c and then compare it with different values of β ($= 0.05, 0.005$, and 0.0005). As seen from the Fig. 5 (b), in our simulation, the rolling coefficient, β , plays the role as of $1/\tau_c$ in Eq. (3). For low values of β , since the chances of cellular rolling/reorganization decreases, sparse branching structure prevails for longer period of time, thus, the coalescence time, τ_c becomes higher. On the other hand, increasing β value increases the rate of coalescence and thus, the cluster compactifies faster.

3.5. Compactness of cellular aggregate

We further investigate how the cellular cohesive strength evolves as the cluster grows in time. In our simulations, it is measured by estimating the adhesion junctions formed between cells, *i.e.*, the total number of bonds formed among the constitutive cells within

the aggregate. As time progresses, the binding strength increases due to more number of cells/clusters joining the aggregate. On the other hand, addition of new cells in the cluster due to diffusion makes the aggregate to spread out. However, aggregates slowly become compact due to local reorganization of cells within the cluster to minimize the binding free energy by forming maximum possible bonds with the neighbouring cells. In our model, we define the compactness of an aggregate, C_r , as total number of bonds in a cluster. It has been, further, normalized to differentiate the increase in number of bonds due to addition of diffusing cells or due to local rearrangement of the relative position of the cells to maximize the binding strength as defined by C_{nr} ,

$$C_{nr} = \frac{\text{Total no. of bonds in a cluster of } n \text{ cells}}{\text{Bonds for making 1D chain of } n \text{ cells}} \quad (4)$$

Thus, C_r has information about the total number of bonds in the aggregate, on the other hand, C_{nr} represents that given a number of cells in an aggregate, how closely cells are packed together.

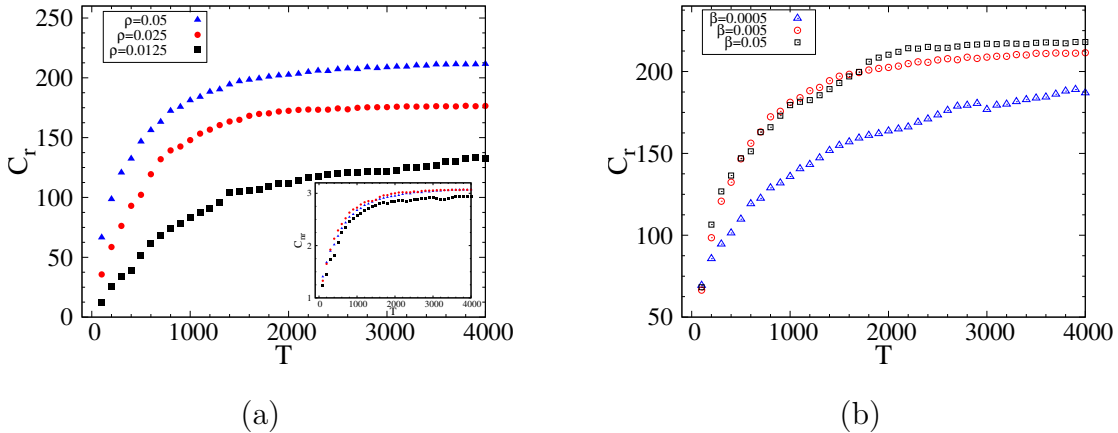


Figure 6. Time evolution of the compactness of cellular aggregate. (a) Shows the effect of different initial cluster density, $\rho = 0.0125$ (■), 0.025 (●), and 0.05 (▲). Corresponding C_{nr} , for different density is shown in inset. (b) Plot shows the dependence of the aggregate compactness on the variation of rolling coefficient for $\beta = 0.0005$ (▲), 0.005 (○), and 0.05 (□).

We have simulated the time evolution of the compactness, C_r , of an aggregate for different cell density, ρ and varying rolling coefficient, β averaged over many aggregates shown in Figs. 6(a) and (b) respectively. As seen from the plot, the compactness, *i.e.*, the binding strength of an aggregate increases as the cluster grows with time. The initial rapid increase is due to joining of diffusing clusters then the increase happens mainly due to the local reorganization of cells that involves breaking and making of new bonds; thus, it occurs at a much slower rate compare to diffusion. Moreover, as cell density increases, the number of cells in an aggregate also increases and hence, the total number of bonds, *i.e.*, compactness also becomes higher. Further, as seen from the inset of Fig. 6(a), since C_{nr} is normalized by the cluster size, all curves for different cell density collapse into a single curve.

3.6. Fractal geometry of the aggregate

Recent studies have shown that the fractal geometry can be useful to understand the underlying mechanisms of tissue growth as living tissues are spatially heterogeneous and thus, exhibit fractal patterns [48]. Moreover, it has been observed that fractal analysis may provide an efficient way to distinguish normal versus cancerous tissue growth. We have, therefore, characterized the fractal dimension of growing aggregates to get insights into the complexity of the structure. In our simulations, the fractal dimension, D , has been estimated from the radius of gyration, R_g , of the evolving cluster using the following relationship [21, 25],

$$R_g \sim n^{1/D}; \quad (5)$$

where n is the number of cells in the cluster. As discussed in the previous section, at early times, the cluster grows due to numerous collisions between the diffusing cells/clusters; thus initially, it develops a branched sparse structure and gradually self-organization of clustering cells gives rise to the compact structure. In our simulations, we start calculating the fractal dimension after the aggregate has grown to a branched structure and then study as time progresses, how the dimension changes due to the compactification process. The time evolution of the fractal dimension, D , averaged over many such aggregates is presented in Fig. 7. As seen from the figure, at the initial stage, the fractal dimension turns out to be similar to the diffusion limited aggregates [21, 22, 51], however, it slowly increases as the clustering cells relocate to the energetically favourable binding sites, and as a result, also compactifies the aggregate. Eventually, the fractal dimension approaches to two for the most compact aggregated structure, as it is expected since the simulation is done on a 2D surface. Moreover, as seen from Fig. 7, with increase in rolling coefficient, β , cluster cells to have higher chances to find their favourable binding sites; thus the compaction process becomes

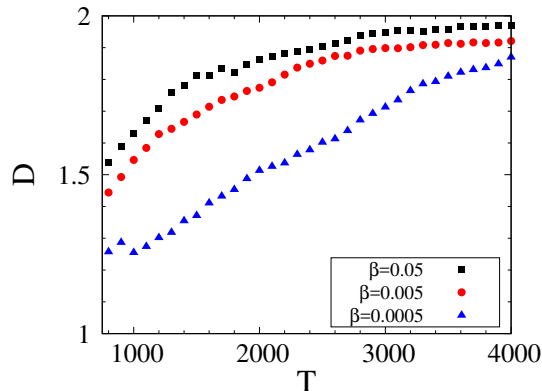


Figure 7. Time variation of fractal dimension of a growing cellular aggregate for different rolling coefficient, $\beta = 0.0005$ (▲), 0.005 (●), and 0.05 (■). Here, the initial cluster density is kept constant at $\rho = 0.05$.

quicker and hence, the fractal dimension of the aggregate also increases faster. On the other hand, it has been observed that the fractal dimension of cancerous tissue increases with increase with progress in cancer stages as the heterogeneity changes due to accumulation of more masses. Interestingly, our study reveals that the difference in the tendency of cell types to increase binding strength also plays a crucial role in determining the structure of the tissue pattern which can be tested further by suitable experiments.

4. Conclusion

We have developed a cellular automata model to study the aggregation dynamics of a seemingly disordered tissue cell population in the absence of any external mediator. This model based on the active motility and local reorganization of cells could successfully capture the structural and temporal evolution of aggregates that leads to the compact tissue structures as observed in experiments. Importantly, our study shows that the sole consideration of the cellular tendency of forming bonds with the neighbouring cells to maximize cohesive strength is sufficient for the spontaneous emergence of compact tissues. Moreover, it provides several insights into the dynamics of the cell aggregation process. It reveals the existence of two distinct time scales - one fast time scale associated with the diffusion of cells and another much slower time scale associated with the tissue compaction process that involves breaking of cell-cell cohesive bonds and making of new bonds leading to local reorganization of cells. Besides, as found in experiments, our simulation results also successfully predicts many dynamical properties of the growing aggregates, such as, the rate of cell aggregation, the non-linear evolution of the surface area, the binding strength and the compactness of the growing aggregate [4, 7, 28]. Moreover, we have demonstrated that the variation in tendency of rolling and reorganization of cells have a profound effect on the formation of tissue shapes and structures and it could be further tested by carrying out suitable experiments. Our theoretical model in essence is of a generic nature and hence can be extended to other systems with suitable modifications. Moreover, since tissue development is quite a complex process and current tissue engineering procedures are still very experimental and also expensive; thus, simple theoretical and computational model studies are envisaged to facilitate the understanding of how individual cells organize into tissues much like as it has been done in passive growth processes which once seemed to be a difficult prospect.

5. Acknowledgments

The authors acknowledge the financial support from Science and Engineering Research Board (SERB), Grant No. SR/FTP/PS-105/2013, Department of Science and Technology (DST), India.

6. References

- [1] Sasai Y. Next-Generation Regenerative Medicine: Organogenesis from Stem Cells in 3D Culture. 2013 *Cell Stem Cell* **12** 520 - 530
- [2] Whitesides GM, Grzybowski B. Self-Assembly at All Scales. 2002 *Science* **295** 2418 -2421
- [3] Jakab K, Norotte C, Marga F, Murphy K, Vunjak-Novakovic G, Forgacs G. Tissue engineering by self-assembly and bio-printing of living cells. 2010 *Biofabrication* **2** 022001
- [4] Gonzalez-Rodriguez D, Guevorkian K, Douezan S, Brochard-Wyart F. Soft Matter Models of Developing Tissues and Tumors. 2012 *Science* **338** 910 -917
- [5] Mironov V, Visconti RP, Kasyanov V, Forgacs G, Drake CJ, Markwald RR. Organ printing: Tissue spheroids as building blocks. 2009 *Biomaterials* **30** 2164 - 2174
- [6] Neagu A, Jakab K, Jamison R, Forgacs G. Role of physical mechanisms in biological self-organization. 2005 *Physical review letters* **95** 178104
- [7] Douezan S, Brochard-Wyart F. Active diffusion-limited aggregation of cells. 2012 *Soft Matter* **8** 784-788
- [8] De R, Zemel A, Safran SA. 2010 Theoretical Concepts and Models of Cellular Mechanosensing. *Methods Cell Biol.* **98** 143-175
- [9] De R. 2018 A general model of focal adhesion orientation dynamics in response to static and cyclic stretch, *Communications Biology* **1** 81
- [10] Ben-Jacob E, Garik P. The formation of patterns in non-equilibrium growth. 1990 *Nature* **343** 523
- [11] Langer JS. Instabilities and pattern formation in crystal growth. 1980 *Rev Mod Phys.* **52** 1-28
- [12] Blando J, Turpin B. Secondary organic aerosol formation in cloud and fog droplets: A literature evaluation of plausibility. 2000 *Atmospheric Environment* **34(10)** 1623-1632
- [13] Weber AP, Baltensperger U, Gggeler HW, Tobler L, Keil R, Schmidt-Ott A. Simultaneous in-situ measurements of mass, surface and mobility diameter of silver agglomerates. 1991 *Journal of Aerosol Science.* **22** S257 - S260
- [14] Bence NF, Sampat RM, Kopito RR. Impairment of the Ubiquitin-Proteasome System by Protein Aggregation. 2001 *Science* **292(5521)** 1552–1555
- [15] Ben-Jacob E, Schochet O, Tenenbaum A, Cohen I, Czirk A, Vicsek T. Generic modelling of cooperative growth patterns in bacterial colonies. 1994 *Nature* **368** 46.
- [16] Matsushita M, Wakita J, Itoh H, Ràfols I, Matsuyama T, Sakaguchi H, et al. Interface growth and pattern formation in bacterial colonies. 1998 *Physica A: Statistical and Theoretical Physics* **249(1-4)** 517-524
- [17] Tsimring L, Levine H, Aranson I, Ben-Jacob E, Cohen I, Shochet O, et al. Aggregation Patterns in Stressed Bacteria. 1995 *Phys Rev Lett.* **75** 1859-1862
- [18] Vicsek T, Zafeiris A. Collective motion. 2012 *Physics Reports.* **517(3)** 71 - 140
- [19] Meakin P. 1998 *Fractals, scaling, and growth far from equilibrium* (Cambridge nonlinear science series 5 Cambridge, U.K. ; New York : Cambridge University Press)
- [20] Barabási AL, Stanley HE. 1995 *Fractal concepts in surface growth* (Cambridge University Press)
- [21] Meakin P. Formation of Fractal Clusters and Networks by Irreversible Diffusion-Limited Aggregation. 1983 *Phys Rev Lett.* **51** 1119-1122
- [22] Witten TA, Sander LM. Diffusion-limited aggregation. 1983 *Phys Rev B.* **27** 5686-5697
- [23] Meakin P. Computer simulation of cluster-cluster aggregation using linear trajectories: Results from three-dimensional simulations and a comparison with aggregates formed using brownian trajectories. 1984 *Journal of Colloid and Interface Science.* **102(2)** 505 - 512
- [24] Vicsek T. Pattern Formation in Diffusion-Limited Aggregation. 1984 *Phys Rev Lett.* **53** 2281-2284
- [25] Kolb M, Botet R, Jullien R. Scaling of Kinetically Growing Clusters. 1983 *Phys Rev Lett.* **51** 1123-1126
- [26] Ryan PL, Foty RA, Kohn J, Steinberg MS. Tissue spreading on implantable substrates is a competitive outcome of cell–cell vs. cell–substratum adhesivity. 2001 *Proceedings of the National Academy of Sciences* **98(8)** 4323-4327

- [27] Douezan S, Guevorkian K, Naouar R, Dufour S, Cuvelier D, Brochard-Wyart F. Spreading dynamics and wetting transition of cellular aggregates. 2011 *Proceedings of the National Academy of Sciences of the United States of America* **108** **18** 7315-20
- [28] Guo Wh, Frey MT, Burnham NA, Wang YL. Substrate Rigidity Regulates the Formation and Maintenance of Tissues. 2006 *Biophysical Journals*. **90**(6) 2213-2220
- [29] Jakab K, Neagu A, Mironov V, Markwald RR, Forgacs G. Engineering biological structures of prescribed shape using self-assembling multicellular systems. 2004 *Proceedings of the National Academy of Sciences* **101**(9) 2864-2869
- [30] Flenner E, Janosi L, Barz B, Neagu A, Forgacs G, Kosztin I. Kinetic Monte Carlo and cellular particle dynamics simulations of multicellular systems. 2012 *Phys Rev E*. **85** 031907
- [31] Graner F, Glazier JA. Simulation of biological cell sorting using a two-dimensional extended Potts model. 1992 *Phys Rev Lett*. **69** 2013-2016
- [32] Beatrici CP and Brunnet LG. Cell sorting based on motility differences. 2011 *Phys Rev E*. **84** 031927
- [33] Tracqui P. Biophysical models of tumour growth. 2009 *Reports on Progress in Physics* **72**(5) 056701
- [34] Steinberg MS. Reconstruction of Tissues by Dissociated Cells. 1963 *Science* **141**(3579) 401-408
- [35] Steinberg MS. Differential adhesion in morphogenesis : a modern view. 2007 *Current Opinion in Genetics & Development* **17**(4) 281-286
- [36] Foty RA, Steinberg MS. The differential adhesion hypothesis: a direct evaluation. 2005 *Developmental Biology* **278**(1) 255 - 263
- [37] Sun Y, Wang Q. Modeling and simulations of multicellular aggregate self-assembly in biofabrication using kinetic Monte Carlo methods. 2013 *Soft Matter* **9** 2172
- [38] Vasiev BN, Hogeweg P and Panfilov AV. Simulation of Dictyostelium Discoideum Aggregation via Reaction-Diffusion Model. 1994 *Phys Rev Lett*. **73** 3173-3176
- [39] Koch W, Friedlander SK. The effect of particle coalescence on the surface area of a coagulating aerosol. 1990 *Journal of Colloid and Interface Science* **140**(2) 419 - 427
- [40] Hiram Y, Nir A. A simulation of surface tension driven coalescence. 1983 *Journal of Colloid and Interface Science* **95**(2) 462- 470
- [41] Vicsek T. Formation of solidification patterns in aggregation models. 1985 *Phys Rev A*. **32** 3084-3089
- [42] Huang SY, Zou XW, Shao ZG, Tan ZJ, Jin ZZ. Particle-cluster aggregation on a small-world network. 2004 *Phys Rev E*. **69** 067104
- [43] Rieu JP and Sawada Y. Hydrodynamics and cell motion during the rounding of two dimensional hydra cell aggregates. 2002 *The European Physical Journal B - Condensed Matter and Complex Systems* **27**(1) 167-172
- [44] Mombach JCM, Robert D, Graner F, Gillet G, Thomas GL, Idiart M, et al. Rounding of aggregates of biological cells: Experiments and simulations. 2005 *Physica A: Statistical Mechanics and its Applications* **352**(2) 525 - 534
- [45] Weijer, Cornelis J. Collective cell migration in development. 2009 *Journal of Cell Science* **122**(18) 3215-3223
- [46] van Oers RFM, Rens EG, LaValley DJ, Reinhart-King CA, Merks RMH Mechanical Cell-Matrix Feedback Explains Pairwise and Collective Endothelial Cell Behavior In Vitro. 2014 *PLOS Computational Biology* **10**(8) 1-14
- [47] Weber, Michele and Hauschild, Robert and Schwarz, Jan and Moussion, Christine and de Vries, Ingrid and Legler, Daniel F. and Luther, Sanjiv A. and Bollenbach, Tobias and Sixt, Michael Interstitial Dendritic Cell Guidance by Haptotactic Chemokine Gradients. 2013 *Science* **339**(6117) 328-332
- [48] Baish, James W. and Jain, Rakesh K. Fractals and Cancer. 2006 *Cancer Research* **60**(14) 3683-3688
- [49] C L Campbell, K Wood, C T A Brown and H Moseley Monte Carlo modelling of photodynamic

- therapy treatments comparing clustered three dimensional tumour structures with homogeneous tissue structures. 2016 *Physics in Medicine & Biology* **61** 4840
- [50] Rob Phillips JT Jane Kondev. 2013 *Physical Biology of the Cell* (Garland Science)
- [51] Sander E, Sander LM and Ziff RM Fractals and Fractal Correlations. 1994 *Comput Phys.* **8(4)** 420-425